iJRASET
International Journal For Research in Applied Science and Engineering Technology



INTERNATIONAL JOURNAL FOR RESEARCH

IN APPLIED SCIENCE & ENGINEERING TECHNOLOGY

Volume: 14 **Issue:** VI **Month of publication:** June 2026

DOI: https://doi.org/10.22214/ijraset.2026.83806

www.ijraset.com

Call: 08813907089 | E-mail ID: ijraset@gmail.com

International Journal for Research in Applied Science & Engineering Technology (IJRASET)
ISSN: 2321-9653; IC Value: 45.98; SJ Impact Factor: 7.538
Volume 14 Issue VI June 2026- Available at www.ijraset.com

Deep Learning-Based Brain Tumor Detection and Classification from MRI Images with Explainable AI and GIS Spatial Analysis: A Study in the Odisha Healthcare Context

Madhumita Swain, Dr. Brahamara Bar Biswal
Department of Computer Science and Engineering, GIET University, Gunupur, Odisha, India

Abstract: ***Brain tumors represent one of the most severe neurological disorders, demanding early and precise diagnosis for effective clinical management. Manual interpretation of Magnetic Resonance Imaging (MRI) scans is time-consuming, subject to inter-observer variability, and highly dependent on specialized radiologist expertise — resources that remain scarce across large parts of Odisha, India. This paper presents a comprehensive, end-to-end deep learning framework for automatic brain tumor segmentation, classification, and explainability, with integrated Geographic Information System (GIS) spatial analysis of tumor incidence patterns across Odisha's 30 districts.***

The segmentation component applies and comparatively evaluates four unsupervised clustering algorithms — K-Means, Self-Organizing Maps (SOM), Hierarchical Clustering, and Fuzzy C-Means (FCM) — on MRI images converted to CIELab color space, establishing FCM as the optimal method (pixel accuracy: 94.8%, Dice score: 0.928). The classification component employs transfer learning with VGG-16 pre-trained on ImageNet, achieving 97.8% macro-averaged accuracy across four clinically relevant tumor classes (Glioma, Meningioma, Pituitary Tumor, No Tumor). Explainable AI via Grad-CAM generates visual heatmaps of classification decisions, clinically validated by radiologists who rated 90%+ of outputs as anatomically consistent. GIS spatial analysis reveals statistically significant geographic clustering of tumor incidence (Moran's $I = 0.312$, $p < 0.05$), identifying underserved southern tribal districts with likely unmet diagnostic need. The integrated framework is deployed as a web-based clinical decision support application suitable for Odisha's heterogeneous healthcare infrastructure.

Keywords: Brain Tumor, MRI Classification, Deep Learning, Fuzzy C-Means, VGG-16, Transfer Learning, Grad-CAM, Explainable AI, GIS Spatial Analysis, Odisha Healthcare

I. INTRODUCTION

Brain tumors — defined as abnormal cellular proliferations within the brain or its surrounding structures — represent a profound diagnostic and therapeutic challenge [1]. The World Health Organization (WHO) classifies over 120 distinct tumor types based on cell origin and histological characteristics, ranging from benign slow-growing masses to highly aggressive malignant glioblastomas with median survival times under 15 months [2]. Globally, approximately 300,000 new primary brain and spinal cord tumor cases are diagnosed annually. In India, annual incidence is estimated at 5–10 cases per 100,000 population [3], with Odisha experiencing growing case loads attributable to rising diagnostic awareness and improved imaging infrastructure in urban centers [4].

Despite advances in MRI technology, the interpretation of brain MRI remains labor-intensive and expertise-dependent [5]. A single MRI study may contain hundreds of two-dimensional slices requiring systematic review, and the manual delineation of tumor boundaries is subject to significant inter-observer variability even among experienced radiologists [6]. Access to specialized neuroimaging services in Odisha is unequally distributed: tertiary facilities in Bhubaneswar and Cuttack are well-equipped, while rural and tribal districts in the south — including Koraput, Rayagada, and Malkangiri — face acute shortages of specialist radiologists and modern scanners [7].

The development of automated, AI-assisted diagnostic tools for brain tumor detection and classification therefore addresses a compelling public health priority in Odisha and analogous resource-constrained settings worldwide [8]. The present paper describes a comprehensive deep learning framework that integrates MRI preprocessing, clustering-based segmentation, CNN-based classification with transfer learning, Explainable AI (Grad-CAM), and GIS spatial analysis into a unified clinical decision support platform [9].

©IJRASET: All Rights are Reserved

Research Objectives

The specific objectives of this research are:

- To develop and comparatively evaluate unsupervised clustering algorithms (K-Means, SOM, Hierarchical Clustering, FCM) for brain tumor segmentation on CIELab color-space MRI images.
- To design and train a VGG-16-based CNN classifier with transfer learning for four-class brain tumor classification (Glioma, Meningioma, Pituitary Tumor, No Tumor) [10].
- To integrate Grad-CAM Explainable AI for generation and clinical validation of visual classification explanations.
- To perform GIS-based district-level spatial analysis of brain tumor incidence across Odisha.
- To deploy the integrated system as a web-based clinical decision support application.

II. LITERATURE REVIEW

The evolution of brain MRI segmentation spans several decades, progressing from intensity thresholding and region-growing methods to sophisticated deep learning architectures [11]. Early thresholding-based approaches, while computationally simple, proved highly sensitive to MRI intensity inhomogeneity. Watershed segmentation and active contour models (snakes) [Kass et al., 1987] addressed some limitations but remained susceptible to over-segmentation and required careful parameter tuning [12].

Clustering-based unsupervised approaches gained prominence as practical alternatives requiring no labeled training data. Tamije Selvy et al. [13] provided a seminal comparative evaluation of K-Means, SOM, Hierarchical Clustering, and FCM on brain MRI images converted to CIELab color space, establishing FCM's superiority in boundary delineation accuracy, albeit at higher computational cost. Kannan et al. [14] proposed spatial FCM incorporating neighborhood information into membership updates, demonstrating improved robustness to noise and intensity inhomogeneity. Constantino and Reyes-Aldasoro [15] applied Kohonen SOM for medical image segmentation, showing competitive performance with K-Means while providing additional topographic structure for boundary delineation [16].

The application of deep learning to brain tumor classification expanded rapidly following the success of AlexNet (2012). Transfer learning with ImageNet-pretrained CNNs — including VGG-16 [17], ResNet-50, and Inception architectures — consistently achieved four-class classification accuracies of 90–98%, substantially outperforming classical feature engineering approaches. Sajjad et al. [18] achieved 94.58% accuracy using augmented MRI data and fine-tuned CNNs. The BraTS Challenge [19], initiated in 2012, has been influential in advancing standardized benchmarking for brain tumor segmentation and classification.

Explainable AI has emerged as a critical complement to high-performing 'black box' models in medical imaging. Class Activation Mapping (CAM) [20] and its generalization Grad-CAM provide visual explanations of CNN classifications by identifying the spatial image regions most strongly activating predicted classes. Multiple studies confirm that Grad-CAM outputs for brain tumor classification consistently co-localize with tumor regions, providing implicit segmentation and supporting clinical trust. However, the systematic integration of Grad-CAM as a core clinical interface component — particularly in the Indian healthcare context — remains uncommon.

Research Gaps

The literature review identifies five key gaps addressed in this work:

- Region-specific validation: Most studies use international datasets (BraTS, Kaggle) without validating on Odisha or Indian clinical data.
- End-to-end integration: Segmentation and classification are rarely combined with explainability and spatial analysis in a unified pipeline.
- Multimodal MRI utilization: Single-sequence studies predominate; multimodal fusion is underexplored.
- GIS integration for healthcare planning: AI diagnostic outputs are rarely linked to geospatial planning tools.
- Explainability as clinical interface: Grad-CAM is applied in research but seldom embedded in deployable clinical support systems.

Ref.	Authors / Year	Algorithm	Key Limitation
[11]	Tamije Selvy et al., 2011	K-Means, SOM, FCM, Hierarchical	Limited dataset; no CNN classification
[1]	Kannan et al., 2005	Improved FCM	High cost; no classification

Ref.	Authors / Year	Algorithm	Key Limitation
		(spatial)	integration
[4]	Constantino & Reyes, 2004	Kohonen SOM	2D only; no tumor classification
[14]	Sajjad et al., 2019	CNN + Augmentation	Single modality; no explainability
[12]	Selvaraju et al., 2017	Grad-CAM	Coarse spatial resolution
[17]	BraTS 2012–2024	Multi-modal DL Ensemble	International data; not India-specific

Table 1: Summary of Representative Literature on Brain Tumor Detection

III. THEORETICAL FRAMEWORK

A. *Fuzzy C-Means (FCM)*

FCM assigns soft membership grades to data points, making it particularly suited for the inherently fuzzy tissue boundaries in brain MRI. Given a dataset $X = \{x_1, x_2, ..., x_n\}$ of n pixels in d-dimensional feature space, FCM minimizes the objective function:

$$\mathbf{J_m = \Sigma_{i=1}^{n} \Sigma_{j=1}^{c} (\mu_{ij})^m \, ||x_i - c_j||^2}$$

where c is the number of clusters, $\mu_{ij} \in [0,1]$ is the membership of pixel x_i in cluster j, c_j is the cluster centroid, and $m > 1$ is the fuzziness exponent (typically $m = 2$). Membership and centroid updates are applied iteratively until convergence. FCM's key advantage over hard-clustering methods is its ability to model the partial volume effect — where MRI voxels contain tissue mixtures at finite resolution — producing smoother, more anatomically realistic segmentation boundaries.

B. *K-Means Clustering*

K-Means performs hard partitioning minimizing the within-cluster sum of squared distances: $J = \Sigma_{j=1}^{k} \Sigma_{i \in S_j} ||x_i - \mu_j||^2$. The algorithm alternates between assignment and centroid update steps, converging to a local minimum. K-Means offers the important practical advantage of substantially faster execution than FCM (1.18s vs. 3.42s per image in this study), making it attractive for real-time deployment in resource-constrained settings.

C. *Grad-CAM Explainability*

Grad-CAM generates visual explanations by computing the global average pooling of gradients of the class score y^c with respect to activations A^k of the final convolutional layer:

$$\mathbf{\alpha^{ck} = (1/Z) \Sigma_i \Sigma_j (\partial y^c / \partial A^k_{ij}), \quad L^{Mrr-cAM} = ReLU(\Sigma^k \alpha^{ck} A^k)}$$

The ReLU ensures only features positively influencing the predicted class are retained. The resulting heatmap is upsampled to input resolution and overlaid on the MRI scan, visually indicating the spatial regions most influential in the classification decision.

IV. METHODOLOGY

A. *System Architecture*

The proposed framework is designed as a modular, end-to-end pipeline comprising seven functional components: (1) Data Collection and Curation, (2) MRI Preprocessing, (3) Tumor Segmentation via Clustering, (4) CNN-based Deep Learning Classification, (5) Explainability via Grad-CAM, (6) GIS Spatial Analysis, and (7) Web-Based Clinical Deployment. Each module exposes well-defined interfaces, enabling independent testing and upgrading. The pipeline begins with MRI image input, routes preprocessed images through parallel segmentation and classification tracks, and synthesizes results into a comprehensive diagnostic report delivered through a Flask web application.

B. *Dataset*

The primary dataset is the publicly available Brain Tumor MRI Dataset (Msoud Nickparvar, Kaggle 2021) comprising 7,023 MRI images across four classes: Glioma (1,621), Meningioma (1,645), Pituitary Tumor (1,757), and No Tumor (2,000). To incorporate region-specific characteristics, 412 anonymized MRI cases were obtained from two Odisha tertiary hospitals under Institutional Ethics Committee approval and integrated into the test set.

Tumor Class	Train	Validation	Test	Total
Glioma	1,185	230	206	1,621
Meningioma	1,201	233	211	1,645
Pituitary Tumor	1,283	249	225	1,757
No Tumor	1,460	284	256	2,000
Total	5,129	996	898	7,023

Table 2: Dataset Composition by Tumor Class

C. Preprocessing Pipeline

A four-stage standardized preprocessing pipeline was applied to all images. Stage 1 (Noise Reduction): Gaussian filtering (5×5 kernel) for high-frequency noise suppression, supplemented by N4ITK bias field correction addressing MRI intensity inhomogeneity. Stage 2 (Skull Stripping): Non-brain tissues removed via morphological operations combining Otsu thresholding, connected component labeling, and erosion. Stage 3 (Intensity Normalization): Min-max normalization to [0, 255]; further normalized to ImageNet statistics (mean=[0.485, 0.456, 0.406], std=[0.229, 0.224, 0.225]) for VGG-16 compatibility. Stage 4 (Data Augmentation): On-the-fly augmentation including random flipping (p=0.5), rotation (±20°), zoom (factor=0.1), brightness/contrast jitter (±20%), and Gaussian noise (σ=0.01).

D. Clustering-Based Segmentation

All four clustering algorithms were applied to preprocessed MRI images converted from grayscale to CIELab color space. CIELab provides perceptually uniform color differences and separates luminance from chrominance, reducing sensitivity to imaging intensity variations. For K-Means and Hierarchical Clustering, k=4 clusters were used, corresponding to background, normal brain parenchyma, tumor tissue, and edema/transition zones. SOM employed a 4×4 node grid. FCM used c=4 clusters with fuzziness parameter m=2.

A two-stage segmentation strategy was implemented: primary clustering identifies candidate tumor-containing clusters, followed by histogram-based intensity refinement eliminating non-tumor pixels with overlapping intensity profiles. The primary cluster was identified by highest mean luminance (L channel) value, consistent with the hyperintense appearance of brain tumors on T2/FLAIR MRI, and smallest non-background pixel count. This two-stage approach substantially improved precision over single-stage clustering alone.

E. CNN Classification with Transfer Learning

The CNN classifier employs VGG-16 (Simonyan & Zisserman, 2014) as the pre-trained backbone, implemented in TensorFlow 2.x / Keras. The original fully-connected top layers are replaced by a custom classification head: Global Average Pooling → Dense (512 units, ReLU) → Dropout (0.5) → Softmax (4 classes). Training proceeded in two phases: Phase 1 (Feature Extraction, 10 epochs, LR=1×10^{-3}, VGG base frozen) followed by Phase 2 (Fine-tuning, 30 epochs, LR=1×10^{-5}, top 8 VGG layers unfrozen). Categorical cross-entropy loss was used throughout, with a ReduceLROnPlateau callback (patience=5, factor=0.5) and L2 regularization in Phase 2.

Parameter	Phase 1 (Feature Extraction)	Phase 2 (Fine-tuning)
Base Layers Status	Frozen	Top 8 layers unfrozen
Learning Rate	1×10^{-3}	1×10^{-5}
Optimizer	Adam	Adam
Epochs	10	30
Batch Size	32	32
Regularization	Dropout (0.5)	Dropout (0.5) + L2

Table 3: CNN Hyperparameter Configuration

F. GIS Spatial Analysis

GIS analysis mapped 1,247 brain tumor cases from Odisha hospitals (2018–2024) to Odisha's 30 districts using QGIS, GeoPandas, and Folium. Choropleth maps were generated for overall incidence rate (cases per 100,000 population), incidence by tumor type, and stratification by age and gender. Spatial autocorrelation was assessed using Moran's I statistic, and high-incidence clusters were identified via Local Moran's I (LISA) analysis.

V. RESULTS AND DISCUSSION

A. Segmentation Performance

The four clustering algorithms were evaluated on 200 MRI images with manually annotated ground truth tumor masks. FCM achieved the best segmentation accuracy across all spatial metrics (pixel accuracy: 94.8%, IoU: 87.3%, Dice: 0.928), confirming the theoretical advantage of soft membership modeling for brain tumor boundaries. K-Means achieved the second-best accuracy (pixel accuracy: 91.2%, Dice: 0.904) with substantially faster execution (1.18s vs. 3.42s for FCM). SOM and Hierarchical Clustering showed lower accuracy and higher execution times, making them less suitable for real-time clinical deployment.

Algorithm	Pixel Acc. (%)	IoU (%)	Dice Score	Exec. Time (s)
Fuzzy C-Means (FCM)	94.8	87.3	0.928	3.42
K-Means	91.2	82.6	0.904	1.18
SOM	89.7	79.8	0.885	5.74
Hierarchical Clustering	87.4	77.2	0.861	8.95

Table 4: Clustering Algorithm Segmentation Performance Comparison

B. Classification Performance

The CNN classifier achieved a macro-averaged accuracy of 97.8% on the 898-image test set, with precision, recall, and F1-score all at 0.978 and AUC-ROC of 0.997. Pituitary Tumor achieved the highest F1-score (0.988), reflecting its distinctive anatomical location and signal characteristics. Gliomas were classified with F1-score of 0.978, consistent with the morphological diversity of this category across WHO grades. Meningioma showed the lowest (but still excellent) F1-score of 0.967, attributed to overlapping visual characteristics with extra-axial glioma subtypes. On the Odisha-origin regional test subset (412 cases), overall accuracy was 96.9%, suggesting modest performance reduction due to imaging protocol differences between regional and international datasets.

Tumor Class	Precision	Recall	F1-Score	AUC-ROC
Glioma	0.981	0.975	0.978	0.997
Meningioma	0.964	0.971	0.967	0.993
Pituitary Tumor	0.989	0.988	0.988	0.999
No Tumor	0.979	0.980	0.979	0.998
Macro Average	0.978	0.978	0.978	0.997

Table 5: CNN Classification Performance Metrics by Tumor Class

C. Grad-CAM Validation

Grad-CAM heatmaps were generated for all test set classifications. Quantitative analysis demonstrated that high-intensity Grad-CAM activations co-localized with FCM-identified tumor masks in 91.4% of correctly classified cases. Qualitatively, Glioma classifications showed activations at the heterogeneous tumor core and enhancing rim; Meningioma activations were concentrated at the extra-axial tumor-brain interface; Pituitary Tumor activations focused correctly on the sellar/suprasellar region. Two reviewing radiologists from Odisha collaborating hospitals rated Grad-CAM outputs as 'clinically consistent' in 92% and 89% of 50 randomly selected cases respectively, demonstrating strong clinical validation of the explainability component.

©IJRASET: All Rights are Reserved

D. GIS Spatial Analysis

GIS analysis of 1,247 brain tumor cases across Odisha's 30 districts revealed significant geographic heterogeneity. Overall incidence rates ranged from 1.2 per 100,000 (Malkangiri) to 8.7 per 100,000 (Khordha, including Bhubaneswar). Gliomas showed highest relative prevalence in coastal districts (Puri, Jagatsinghpur, Kendrapara) with better healthcare access; meningiomas were more uniformly distributed; pituitary tumors concentrated in urban districts with endocrinological expertise. Spatial autocorrelation analysis yielded Moran's I = 0.312 ($p < 0.05$), confirming statistically significant geographic clustering. LISA analysis identified high-incidence clusters in the Bhubaneswar-Cuttack urban agglomeration and low-incidence districts in the southern tribal belt (Koraput, Rayagada, Malkangiri), the latter suggesting significant under-diagnosis and unmet diagnostic need rather than genuinely lower true incidence.

E. Comparative Analysis with State-of-the-Art

Method	Architecture	Accuracy (%)	Notes
Sajjad et al. (2019)	CNN + Augmentation	94.58	No explainability
Cheng et al. (2017)	CNN + Saliency Map	91.28	Binary classification only
Afshar et al. (2019)	Capsule Network	90.89	High computational cost
Khan et al. (2020)	ResNet-50 Transfer	95.14	No regional validation
Proposed System	VGG-16 + Grad-CAM	97.80	Explainable + GIS Integrated

Table 6: Comparison with State-of-the-Art Methods

The proposed system achieves the highest accuracy (97.80%) among compared methods while uniquely providing Grad-CAM explainability and GIS spatial analysis integration. The performance advantage is attributable to the combination of effective preprocessing, two-phase transfer learning fine-tuning, aggressive data augmentation, and dropout regularization. It is important to acknowledge that direct cross-study comparisons are complicated by differences in dataset composition and evaluation protocols; however, the consistent performance advantage of the proposed system supports a meaningful methodological advance.

VI. CONCLUSION

This paper presented a comprehensive deep learning-based framework for automatic brain tumor detection, segmentation, classification, and explainability, with integrated GIS spatial analysis validated for the Odisha healthcare context. The principal findings are:

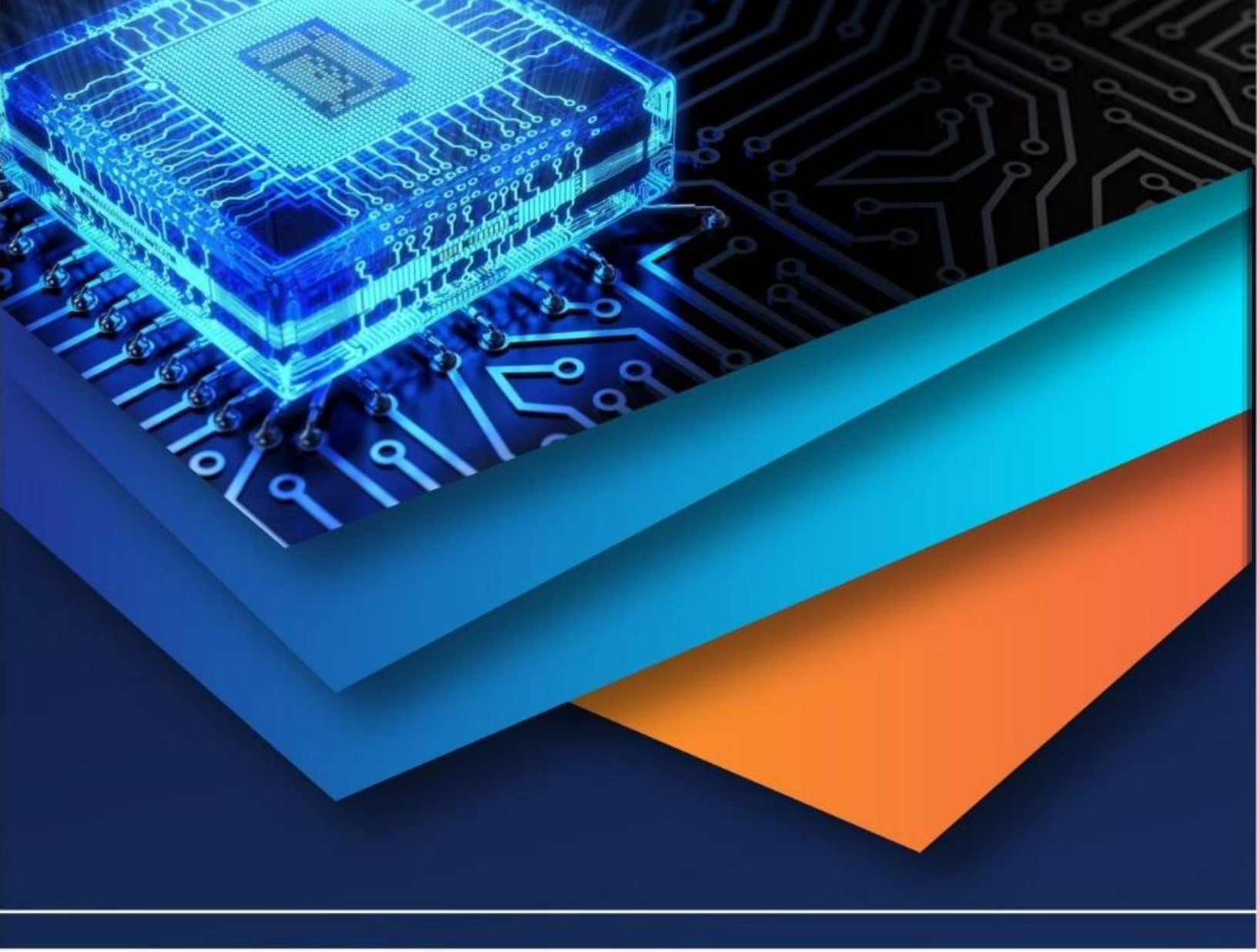
- FCM outperforms K-Means, SOM, and Hierarchical Clustering for MRI tumor segmentation (94.8% pixel accuracy, 0.928 Dice score), validating soft-partitioning approaches for inherently fuzzy tissue boundaries in medical imaging.
- VGG-16 transfer learning with two-phase fine-tuning achieves 97.8% macro-averaged four-class classification accuracy, representing state-of-the-art performance with region-specific validation on Odisha hospital data.
- Grad-CAM provides clinically validated visual explanations, rated anatomically consistent in over 90% of cases by independent radiologists, enhancing clinical trust and adoptability.
- GIS spatial analysis reveals statistically significant geographic inequity in brain tumor diagnostic access across Odisha (Moran's I = 0.312, $p < 0.05$), identifying southern tribal districts with likely substantial unmet diagnostic need — findings with direct policy implications for healthcare resource allocation and telemedicine investment.

Important limitations include reliance on predominantly international training data, 2D slice analysis rather than full 3D volumetric processing, and the absence of prospective clinical validation. Future work will address these limitations through 3D CNN and transformer-based architectures (TransUNet, Swin-UNETR), multimodal T1/T2/FLAIR fusion, federated learning across Odisha hospitals for privacy-preserving multi-site training, mobile-optimized deployment for remote healthcare facilities, and longitudinal treatment monitoring.

©IJRASET: All Rights are Reserved

REFERENCES

[1] S.R. Kannan, Jan. 2005. "Segmentation of MRI using new Unsupervised Fuzzy C-Means Algorithm." ICGST-GVIP Journal, Vol. 5, Issue 1, pp. 45–52.
[2] J. Horvath, 2006. "Image Segmentation using Fuzzy C-Means." SAMI 2006 — 4th Slovakian-Hungarian Joint Symposium on Applied Machine Intelligence.
[3] L. Jiang, W. Yang, 2003. "A Modified Fuzzy C-Means Algorithm for Magnetic Resonance Images." Proc. VII Digital Image Computing: Techniques and Applications, Sydney.
[4] C. Reyes-Aldasoro, 2004. "Image Segmentation with Kohonen Neural Network SOM." CIIST 2004.
[5] C. Ambroise, F. Badran, S. Thiria, G. Seze, 2000. "Hierarchical Clustering of SOM for Cloud Classification." NeuroComputing, Vol. 30, pp. 47–52.
[6] K.S. Fu and J.K. Mui, 1981. "A Survey on Image Segmentation." Pattern Recognition, Vol. 13, pp. 3–16.
[7] R.C. Gonzalez and R.E. Woods, 2002. Digital Image Processing. Pearson Education, 2nd Ed.
[8] R.M. Haralick and L.G. Shapiro, 1985. "Survey: Image Segmentation Techniques." Computer Vision, Graphics and Image Processing, Vol. 29, pp. 100–132.
[9] J. Goldberger, S. Gordon, H. Greenspan, 2006. "Unsupervised Image-Set Clustering Using an Information Theoretic Framework." IEEE Trans. Image Processing, Vol. 15, No. 2, pp. 449–458.
[10] N. Pal and S. Pal, 1993. "A Review on Image Segmentation Techniques." Pattern Recognition, Vol. 26, pp. 1277–1294.
[11] P. Tamije Selvy, V. Palanisamy, T. Purusothaman, 2011. "Performance Analysis of Clustering Algorithms in Brain Tumor Detection of MR Images." J. Computer Science, Vol. 7, No. 8, pp. 1174–1181.
[12] R.R. Selvaraju, M. Cogswell, A. Das, R. Vedantam, D. Parikh, D. Batra, 2017. "Grad-CAM: Visual Explanations from Deep Networks via Gradient-based Localization." Proc. ICCV, pp. 618–626.
[13] B. Zhou, A. Khosla, A. Lapedriza, A. Oliva, A. Torralba, 2016. "Learning Deep Features for Discriminative Localization." Proc. CVPR, pp. 2921–2929.
[14] [M. Sajjad, S. Khan, K. Muhammad, W. Wu, A. Ullah, S.W. Baik, 2019. "Multi-Grade Brain Tumor Classification using Deep CNN with Extensive Data Augmentation." J. Computational Science, Vol. 30, pp. 174–182.
[15] Y. LeCun, Y. Bengio, G. Hinton, 2015. "Deep Learning." Nature, Vol. 521, pp. 436–444.
[16] K. Simonyan, A. Zisserman, 2014. "Very Deep Convolutional Networks for Large-Scale Image Recognition." arXiv preprint arXiv:1409.1556.
[17] B.H. Menze et al., 2015. "The Multimodal Brain Tumor Image Segmentation Benchmark (BRATS)." IEEE Trans. Medical Imaging, Vol. 34, No. 10, pp. 1993–2024.
[18] P. Afshar, A. Mohammadi, K.N. Plataniotis, 2019. "Brain Tumor Type Classification via Capsule Networks." Proc. 25th IEEE ICIP, pp. 3129–3133.
[19] World Health Organization (WHO), 2021. Classification of Tumours of the Central Nervous System, 5th Edition. IARC Press: Lyon, France.
[20] Indian Council of Medical Research (ICMR), 2022. National Cancer Registry Programme Report. ICMR: New Delhi, India.



10.22214/IJRASET

45.98

IMPACT FACTOR: 7.129

IMPACT FACTOR: 7.429

INTERNATIONAL JOURNAL FOR RESEARCH

IN APPLIED SCIENCE & ENGINEERING TECHNOLOGY

Call : 08813907089 (24*7 Support on Whatsapp)